physiologia

MDPI

Article

Effects of Chronic Stress Exposure on Bone Structure and Calcium and Phosphorus Metabolism in Rats

Jean Marc Pujo [1,*], Latifa Hamdaoui [2,†], Marwa Lakhrem [3,†], Dewi Yunia Fitriani [4,5,6], Hajer Ben Saad [3], Ons Boudawara [7], Tahia Boudawara [7], Majed Kammoun [3], Hatem Kallel [8,9,‡] and Ibtissem Ben Amara [3,9,‡]

1 Emergency Department, Cayenne General Hospital, Cayenne 97309, French Guiana
2 Laboratory of Induced and Development Diseases (LR19ES12), Medicine Faculty of Sfax University, Sfax 6000, Tunisia; latifa.hamdaoui20@gmail.com
3 Laboratory of Medicinal and Environmental Chemistry, Higher Institute of Biotechnology, University of Sfax, P.O. Box 261, Sfax 3000, Tunisia; lakhremma@gmail.com (M.L.); hajer.ben.saad@hotmail.fr (H.B.S.); majed.kammoun@gmail.com (M.K.); ibtissem.benamara@isbs.usf.tn (I.B.A.)
4 Community Medicine Department, Faculty of Medicine, Universitas Indonesia, Jakarta 10430, Indonesia; dewi.yunia.fitriani@gmail.com
5 Occupational Medicine Specialist Program, Faculty of Medicine, Universitas Indonesia, Jakarta 10430, Indonesia
6 Occupational and Environmental Health Research Center, Indonesian Medical Education and Research Institute, Faculty of Medicine, Universitas Indonesia, Jakarta 10430, Indonesia
7 Laboratory of Anatompathology, CHU Habib Bourguiba, University of Sfax, Sfax 3029, Tunisia; annoussa1988@gmail.com (O.B.); tahya.sellami61@gmail.com (T.B.)
8 Intensive Care Unit, Cayenne General Hospital, Cayenne 97300, French Guiana; kallelhat@gmail.com
9 Institut Santé des Populations en Amazonie INSERM UA17, Centre Hospitalier Universitaire de Guyane-Site de Cayenne, Université de Guyane, Cayenne 97306, French Guiana
* Correspondence: tamac1966@gmail.com
† These authors contributed equally to this work.
‡ These authors also contributed equally to this work.

Abstract

Objective: This study investigated the effects of three chronic stress exposure models (permanent elimination, forced swimming, and food and water deprivation) on bone oxidative stress, structure, and metabolism *in vivo*. **Methods:** Adult rats were exposed to different stress conditions, while control animals were maintained under standard laboratory conditions. Bone morphological and histological parameters, oxidative stress biomarkers, antioxidant defense system, and mineral concentrations were assessed. **Results:** Stress exposure resulted in significant reductions in body weight, femur weight, and femur length compared to controls. A marked increase in oxidative stress biomarkers was observed in bone tissue, including lipid peroxidation, reactive oxygen species, hydroperoxides, hydrogen peroxide, protein carbonyls, and advanced oxidation protein products. In contrast, antioxidant defenses, including enzymatic activities and levels of glutathione, non-protein thiols, and vitamin C, was significantly decreased. Bone calcium and phosphorus levels were reduced, whereas their plasma concentrations were increased following stress exposure. Histological analysis confirmed the biochemical alterations, suggesting that chronic stress can disrupt bone integrity via oxidative mechanisms. **Conclusions:** These findings highlight the need for strategies to control and reduce stress-related disorders to maintain skeletal health under various chronic stress conditions.

Keywords: light stress; forced swim stress; food and water stress; mineral composition; bone

Check for updates

Academic Editor: Philip J. Atherton

Received: 16 April 2026
Revised: 18 June 2026
Accepted: 23 June 2026
Published: 17 July 2026

Copyright: © 2026 by the authors. Licensee MDPI, Basel, Switzerland. This article is an open access article distributed under the terms and conditions of the Creative Commons Attribution (CC BY) license.

1. Introduction

Bone is a specialized connective tissue that provides structural support and mechanical strength to the body. Bone tissue is constantly renewed through a balance between formation and resorption, involving three cell types: osteocytes, osteoblasts, and osteoclasts [1,2]. Osteoblasts are responsible for synthesizing, secreting, and mineralizing the bone matrix [3]. Once embedded in the matrix, osteoblasts become osteocytes, which play a key role in bone remodeling [4]. Osteoclasts, which originate from monocyte/macrophage lineage precursors, are the primary cells responsible for bone resorption. Bone remodeling is generally described as a sequence of activation, resorption, reversal, and formation phases. This process requires interaction among growth factors, cytokines, and hormones. Over approximately six months, osteoclasts remove old or damaged bone tissue, while osteocytes help transmit signals that regulate mechanical load adaptation.

Numerous factors can adversely affect bone metabolism and skeletal maturation, leading to oxidative stress and cellular damage [5–7]. Oxidative stress arises from an imbalance between antioxidants and excessive production of reactive oxygen species (ROS) [8]. By inducing osteocyte and osteoblast death, this imbalance can prevent bone mineralization and osteogenesis. These mechanisms accelerate bone loss and contribute to osteoporosis by disrupting the balance between bone formation and resorption [9].

Chronic stress exposure can arise from diverse conditions that affect physiological homeostasis via distinct biological pathways. It can alter endocrine regulation, energy metabolism, and oxidative balance. In the present study, three well-established experimental stress models were selected because they represent distinct physiological domains of chronic stress, as previously reported [10–14]. Food and water deprivation reflect a metabolic and nutritional stress [15]. Permanent illumination represents a model that reflects circadian and environmental-related stress [16]. The forced swimming model represents physiological and psychological stress by activating stress response pathways. Although these stressors have been investigated individually in experimental models [12], their comparative effects on bone metabolism remain poorly understood. Comparing these distinct forms of chronic stress may therefore help determine whether they induce common alterations in bone homeostasis through shared mechanisms, such as oxidative stress, or whether they produce stressor-specific skeletal responses. This study therefore aimed to investigate the effects of permanent illumination, forced swimming, and food and water deprivation on oxidative stress, mineral composition, and histopathological changes in the bones of adult rats.

2. Results

2.1. Effects of Chronic Stress Exposure on Body Weight, Femur Weight, and Length in Adult Rats

The results in Figure 1 show that body weight decreased by 29, 23, and 15% in the FW, PI, and FS groups, respectively, compared with controls (Figure 1A). The effects observed in the FW group were significantly more pronounced than those of PI and FS ($p < 0.001$). In contrast, FS resulted in the smallest reduction (FS vs. PI, $p < 0.001$). Femur weight and length were reduced by 42, 48, and 39%, and by 6, 9, and 9% in the FW, PI, and FS groups, respectively, compared with controls (Figure 1B). The most severe effect on femoral mass was observed in the PI group (PI vs. FW and FS, $p < 0.001$). Regarding length, FW showed a significantly smaller decrease than PI and FS (FW vs. PI and FS, $p < 0.001$).

2.2. Effects of Chronic Stress Exposure on Mineral Content in Plasma and Femurs

Different forms of chronic stress, especially food and water deprivation, altered the mineral composition of plasma and femurs, including calcium, phosphorus, iron, zinc, magnesium, and copper. Most minerals decreased in plasma and bone tissue; however,

plasma calcium levels increased significantly across the three stress paradigms employed in this study: food and water restriction, continuous light exposure, and forced swimming (Table 1).

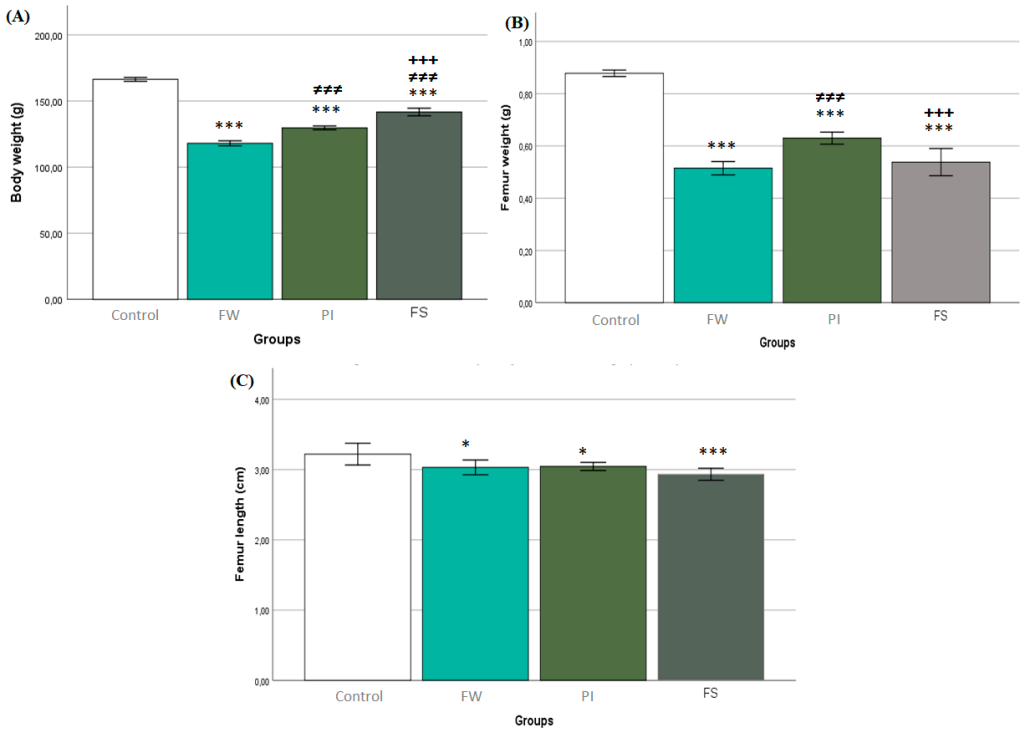


Figure 1. Body weight (**A**), femur weight (**B**), and femur length (**C**) in control, food and water restriction (FW), permanent illumination (PI), and forced swimming (FS) groups after 21 days of exposure. Values are expressed as mean ± SD. Error bars represent the 95% confidence interval. The FW, PI, and FS groups differed significantly from the control group (* $p < 0.05$; *** $p < 0.001$). The FW group differed significantly from the PI and FS groups (≠≠≠ $p < 0.001$). The PI group differed significantly from the FS group (+++ $p < 0.001$).

Table 1. Mineral contents in plasma and femurs of adult rats from the control, food and water restriction (FW), permanent illumination (PI), and forced swimming (FS) groups after 21 days of exposure.

		Control	FW	PI	FS
Femurs (mg/g)	Calcium	140 ± 1.22	60 ± 1.14 ***	80 ± 1.89 ***≠≠≠	70 ± 1.78 ***≠≠≠++
	Phosphorus	55 ± 1.26	28 ± 1.41 ***	45 ± 1.58 ***≠≠≠	38 ± 2.09 ***≠≠≠+
	Iron	0.95 ± 0.01	0.34 ± 0.01 ***	0.4 ± 0.12 ***	0.38 ± 0.03 ***
	Zinc	1.40 ± 0.14	0.7 ± 0.13 ***	0.9 ± 0.08 ***≠	0.85 ± 0.01 ***≠
	Magnesium	40 ± 1.44	30 ± 1.92 ***	36 ± 2.19 ***≠	34 ± 2.09 ***≠
	Copper	0.50 ± 0.14	0.20 ± 0.09 ***	0.4 ± 0.12 ***	0.27 ± 0.02 ***
Plasma (mg/L)	Calcium	62 ± 0.89	90 ± 2.98 ***	78 ± 2.44 ***≠	80 ± 1.87 ***≠
	Phosphorus	90 ± 1.67	35 ± 1.04 ***	40 ± 4.38 ***	48 ± 7.12 ***≠≠+
	Iron	0.18 ± 0.01	0.11 ± 0.01 **	0.10 ± 0.012 ***	0.15 ± 0.008 **≠≠++
	Zinc	0.08 ± 0.01	0.05 ± 0.01 ***	0.07 ± 0.011 **	0.07 ± 0.01 **≠≠++
	Magnesium	0.55 ± 0.12	0.23 ± 0.01 ***	0.30 ± 0.04 ***	0.28 ± 0.02 ***
	Copper	0.02 ± 0.01	0.012 ± 0.001 ***	0.018 ± 0.008 ***	0.011 ± 0.001 ***

Values were expressed as mean ± SD. The FW, PI, and FS groups differed significantly from the control group (** $p < 0.01$; *** $p < 0.001$). The FW group differed significantly from the PI and FS groups (≠ $p < 0.05$; ≠≠ $p < 0.01$; ≠≠≠ $p < 0.001$). The PI group differed significantly from the FS group (+ $p < 0.05$; ++ $p < 0.01$).

FW was the most detrimental stress condition for most minerals, followed by FS, while PI caused more moderate decreases. Intergroup comparisons revealed that FW differed significantly from PI and FS in terms of calcium, phosphorus, zinc, and magnesium ($p < 0.001$). Additionally, FS showed a significant difference from PI regarding calcium and phosphorus ($p < 0.05$).

2.3. Effects of Chronic Stress Exposure on Plasma Levels of Acid and Alkaline Phosphatases

Plasma ACP increased by 65% in the FW group, 10% in the PI group, and 40% in the FS group compared to the controls (Figure 2). The increase was significantly greater in the FW group than in the other two groups (FW vs. PI and FS, $p < 0.001$). In contrast, ALP levels decreased by 16% in FW, 6% in PI, and 7% in FS, with the FW group showing the largest decrease and FS showing an intermediate decrease (FW vs. PI and FS, $p < 0.001$; FS vs. PI, $p < 0.001$).

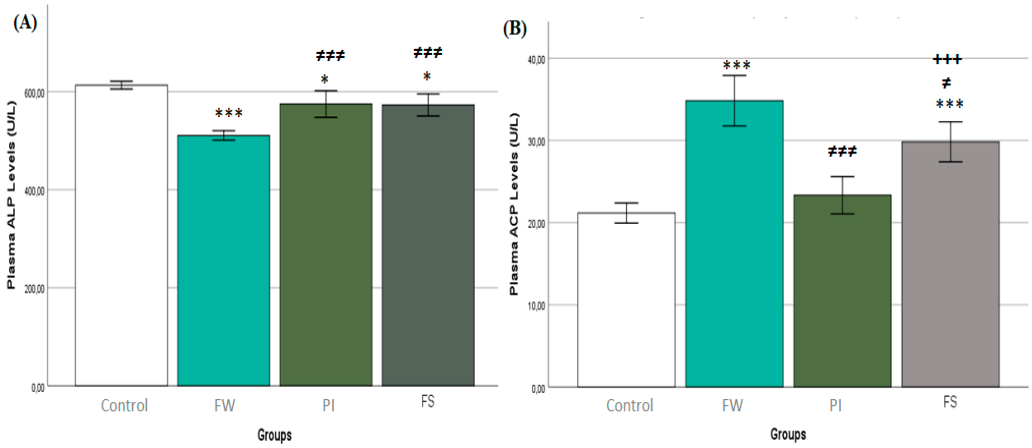


Figure 2. Plasma levels of total alkaline phosphatase (ALP) (**A**) and total tartrate-resistant acid phosphatase (ACP) (**B**) of adult rats from control, food and water restriction (FW), permanent illumination (PI), and forced swimming (FS) groups after 21 days of exposure. Values are expressed as mean ± SD. Error bars represent the **95%** confidence interval. The FW, PI, and FS groups differed significantly from the control group (* $p < 0.05$; *** $p < 0.001$). The FW group differed significantly from the PI and FS groups ($\neq$ $p < 0.05$; $\neq\neq\neq$ $p < 0.001$). The PI group differed significantly from the FS group (+++ $p < 0.001$).

2.4. Effects of Chronic Stress on Oxidative Stress Parameters

All oxidative stress markers, specifically MDA, LOOH, ROS, H_2O_2, AOPP, and PCO, were significantly elevated in the FW, PI, and FS groups compared to controls ($p < 0.001$). The FW group exhibited the highest levels of oxidative damage, significantly greater than those observed in both the PI and FS groups ($p < 0.001$). Additionally, the FS group demonstrated significantly higher oxidative stress levels than the PI rats ($p < 0.001$). These findings indicate that food and water restriction resulted in the most severe oxidative damage, followed by forced swimming and permanent illumination (Figure 3).

2.5. Enzymatic and Non-Enzymatic Antioxidant Defense in Bone

The activities of the enzymes SOD, CAT, and GPx decreased significantly in the different treatment groups compared to the control. In the FW group, enzyme activities decreased by 30, 56, and 27%, respectively. In the PI group, the reductions were 20%, 18%, and 14%, respectively, and in the FS group, the decreases were 27, 49, and 13%, respectively. Among these groups, FW exhibited a significantly greater impairment than both PI and FS ($p < 0.001$), while FS was slightly more affected than PI ($p < 0.01$).

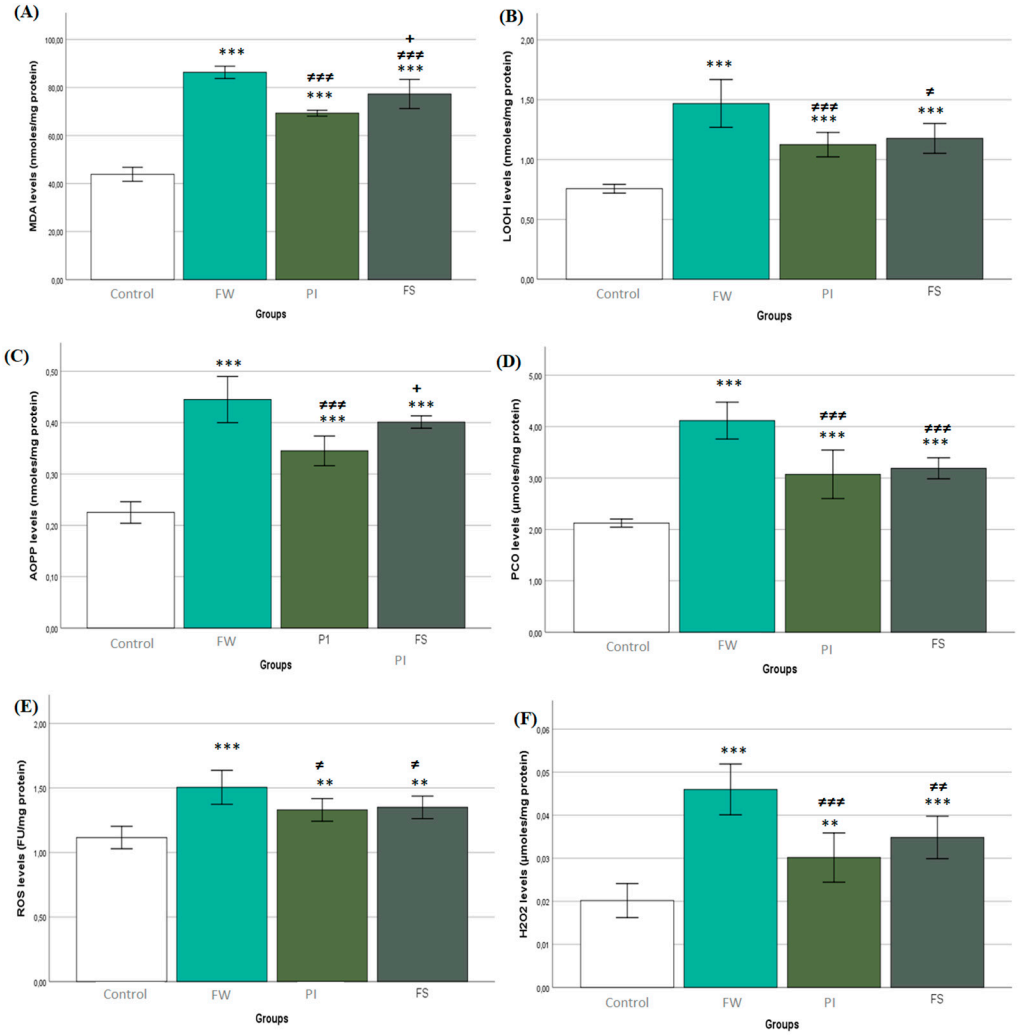


Figure 3. Malondialdehyde (MDA) (**A**), lipid hydroperoxides (LOOHs) (**B**), advanced oxidation protein products (AOPP) (**C**), protein carbonyl (PCO) (**D**), reactive oxygen species (ROS) (**E**), and hydrogen peroxide (H_2O_2) (**F**) levels in the bone of adult rats from control, food and water restriction (FW), permanent illumination (PI), and forced swimming (FS) groups after 21 days of exposure. Values are expressed as mean ± SD. Error bars represent the **95%** confidence interval. The FW, PI, and FS groups differed significantly from the control group (** $p < 0.01$; *** $p < 0.001$). The FW group differed significantly from the PI and FS groups ($\neq$ $p < 0.05$; $\neq\neq$ $p < 0.01$; $\neq\neq\neq$ $p < 0.001$). The PI group differed significantly from the FS group (+ $p < 0.05$).

The results of non-enzymatic antioxidant defenses showed significant decreases in GSH, NPSH, and vitamin C levels in femoral extracts, respectively, from FW (23, 35, and 42%, $p < 0.001$), PI (11, 24, and 43%, $p < 0.01$), and FS (11, 14, and 36%, $p < 0.001$) chronic-stress-exposed groups, compared with controls (Figure 4).

2.6. Scanning Electron Microscopy (SEM) Results

The trabecular bone in the control group exhibited a homogeneous structure (Figure 5A,A1–A3). However, rats exposed to the three stress paradigms employed in this study: food and water restriction, continuous light exposure, and forced swimming, showed trabecular separation at the extremities and thinning of the trabecular bone. These observations were more pronounced, particularly in the FW group (Figure 5B,B1–B3). The endosteum (neocortical) of rats exposed to the three chronic stress conditions showed a decrease in the osteon area (Figure 5C1–C3,D1–D3). The qualitative SEM observations were supported by the histomorphometric analysis of trabecular separation (Figure 5E). A sig-

nificant increase in intertrabecular distance was observed in all stressed groups compared with controls, confirming the deterioration of trabecular bone microarchitecture induced by chronic stress (Figure 5E).

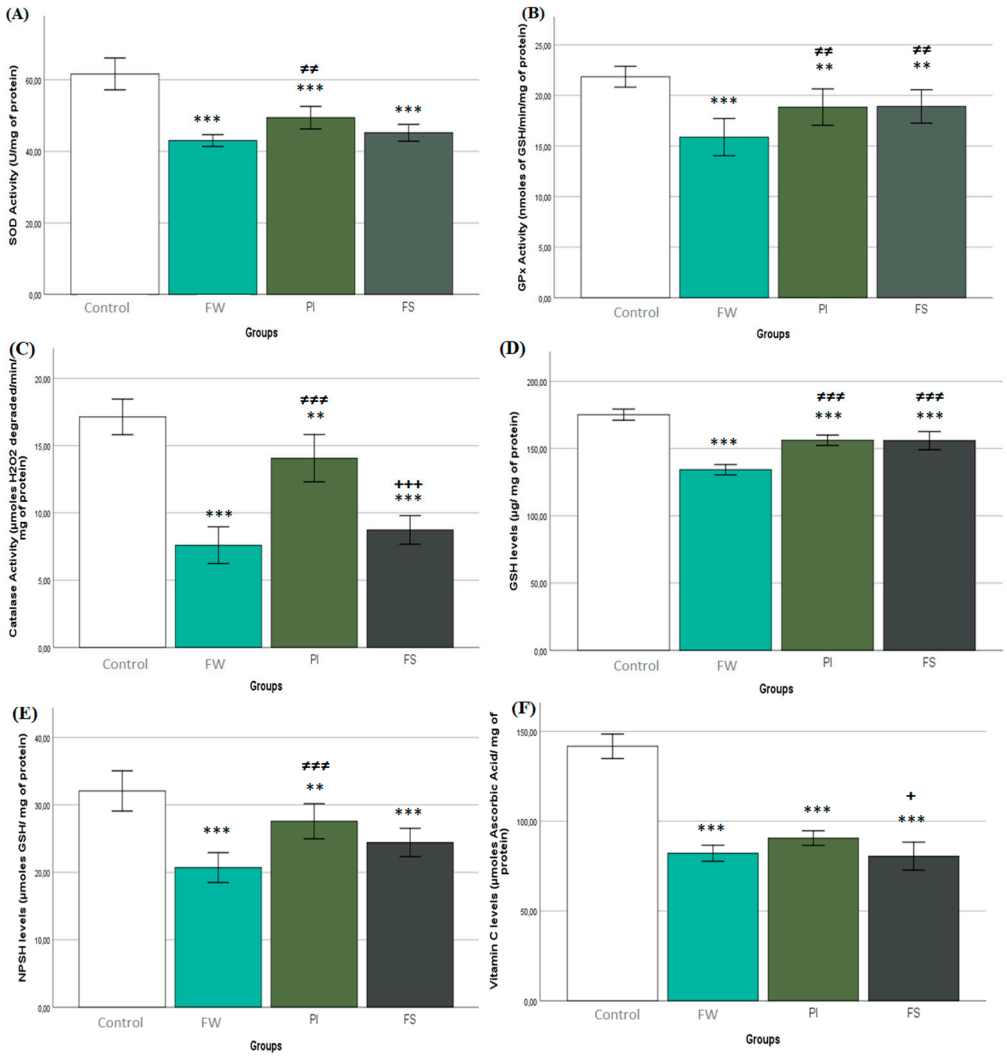


Figure 4. Enzymatic activities of superoxide dismutase (SOD) (**A**), glutathione peroxidase (GPx) (**B**), catalase (CAT) (**C**), glutathione (GSH) (**D**), non-protein sulfhydryls (NPSH) (**E**), and vitamin C (**F**) levels in the bone of adult rats from control, food and water restriction (FW), permanent illumination (PI), and forced swimming (FS) groups after 21 days of exposure. Values are expressed as mean ± SD. Error bars represent the **95%** confidence interval. The FW, PI, and FS groups differed significantly from the control group (** $p < 0.01$; *** $p < 0.001$). The FW group differed significantly from the PI and FS groups ($\neq\neq$ $p < 0.01$; $\neq\neq\neq$ $p < 0.001$). The PI group differed significantly from the FS group (+ $p < 0.05$; +++ $p < 0.001$).

2.7. Histological Bone Analyses

Hematoxylin–Eosin staining showed normal organization of the femoral growth plate in control rats and in the other groups (Figure 6A1,A2). Histological analysis revealed thinning and discontinuity of trabecular bone, along with decreased connectivity and thinning of trabeculae, in the food- and water-deprived group (Figure 6B1,B2). This trabecular bone discontinuity indicates severe decalcification. Moreover, histological sections from the group exposed to stress illumination showed well-developed bone trabeculae with dark coloration, indicating a mineralization defect (Figure 6C1,C2). The bone trabeculae were well developed in the swim stress group but exhibited basophilic coloration, indi-

cating a mineralization defect (Figure 6D1,D2). Histomorphometric data confirmed these histological observations.

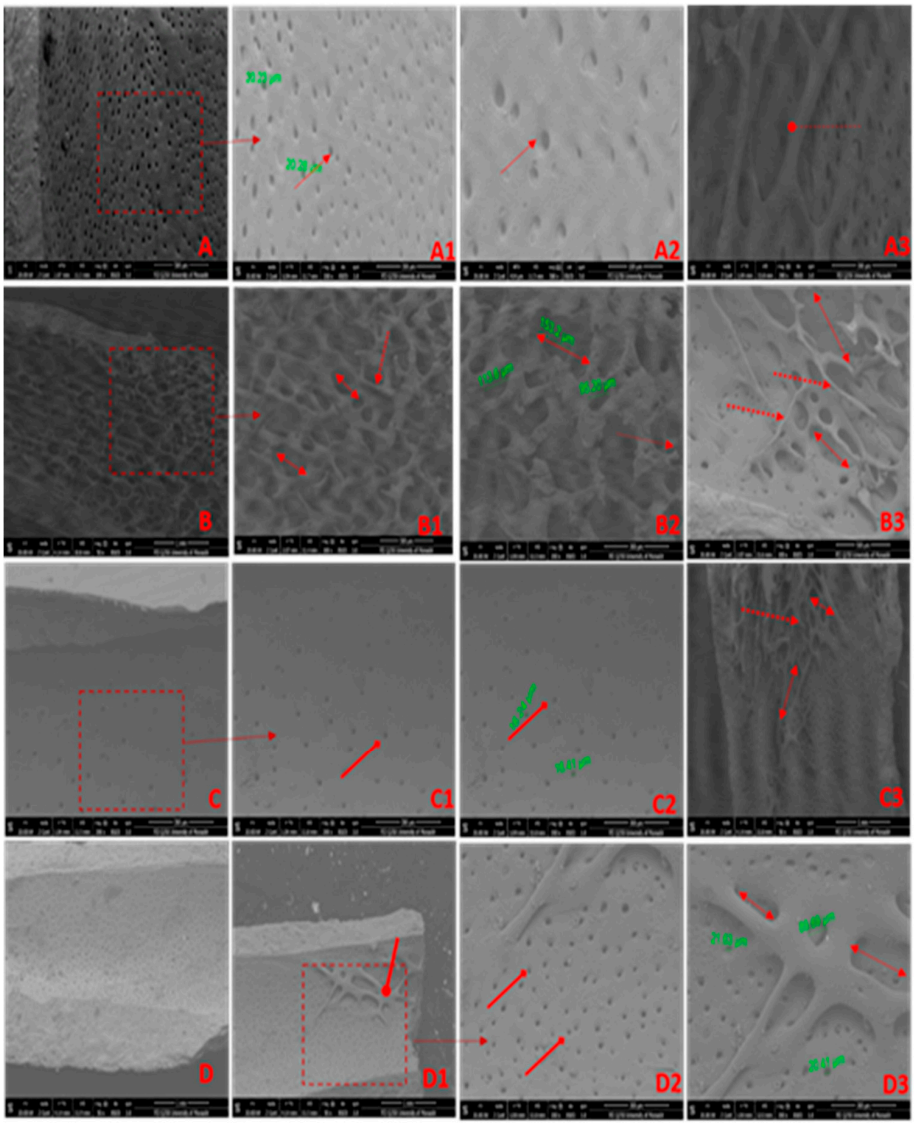


Figure 5. Scanning Electron Microscopy (SEM) micrographs of femurs from control (**A**,**A1**–**A3**), femurs from food and water deprivation (FW) group (**B**,**B1**–**B3**), femurs from permanent illumination

(PI) group (**C**,**C1**–**C3**), and femurs from forced swim (FS) group (**D**,**D1**–**D3**). Original magnification: 100×, 300× and 500×. (**E**): Histomorphometric analysis of intertrabecular distance in trabecular bone in different groups. Values are expressed as mean ± SD. Error bars represent the **95%** confidence interval. The FW, PI, and FS groups differed significantly from the control group (*** $p < 0.001$). No significant differences were observed among the FW, PI and FS groups.

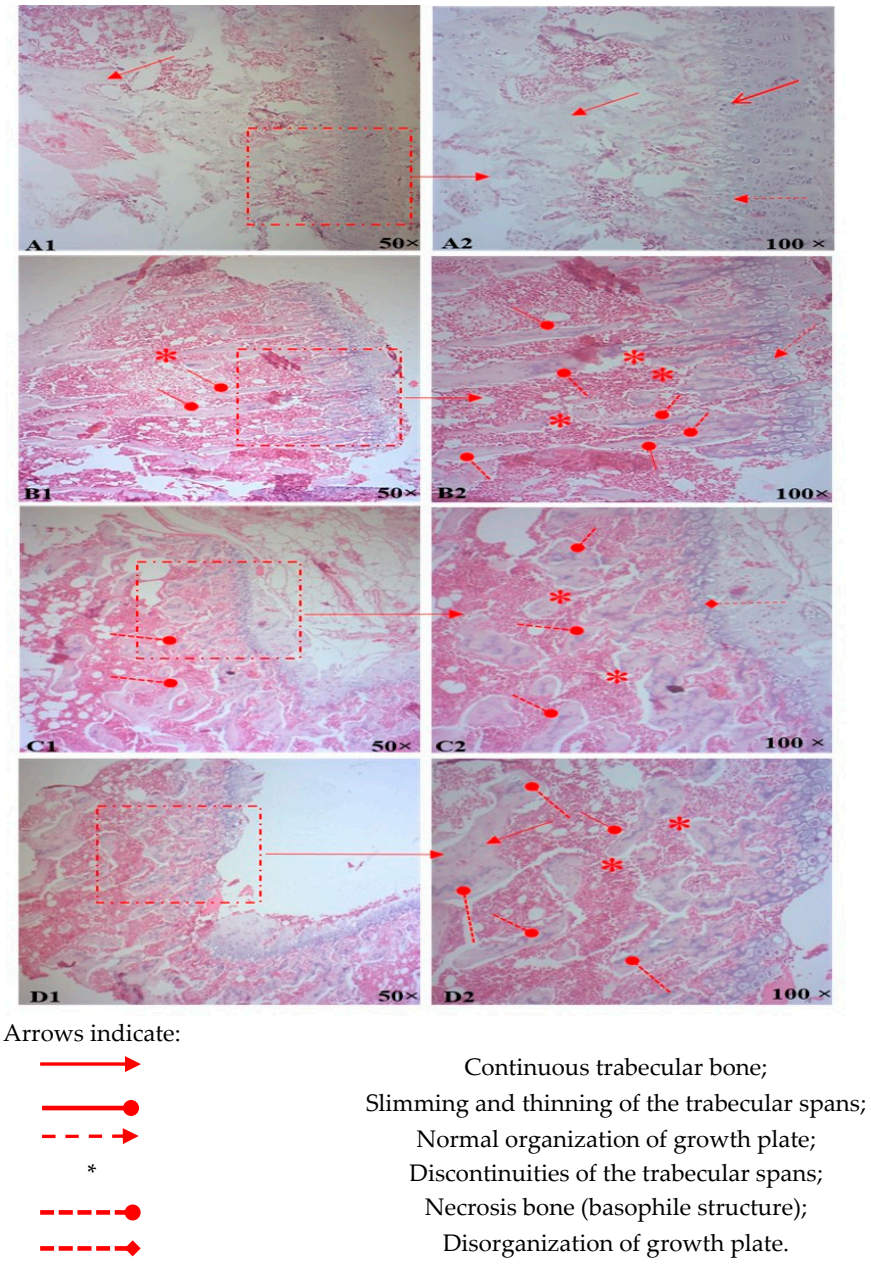


Figure 6. Hematoxylin–Eosin–stained sections of distal femurs (Epiphysis) from control (**A1**,**A2**), food and water deprivation (FW) group (**B1**,**B2**), permanent illumination (PI) group (**C1**,**C2**), and forced swim (FS) group (**D1**,**D2**)—original magnification of H-E stain (200× and 400×).

2.8. Histomorphometric Findings

Histomorphometric analysis showed significant changes in femoral tissue in animals exposed to chronic stress for 21 days compared with controls (Table 2). Exposure to experimental stress models resulted in significant decreases in osteoid surface area of 42, 55, and 53% in the FW, PI, and FS groups, respectively, and in trabecular thickness. Trabecular bone volume increased in the forced swim group, and trabecular number increased across

the different experimental stress groups. Additionally, histomorphometric findings showed an increased intertrabecular distance.

Table 2. Histomorphometric findings in adult rats from the control, food and water restriction (FW), permanent illumination (PI), and forced swimming (FS) groups after 21 days of exposure.

Parameter	Control	FW	PI	FS
(BV/TV) (%)	53.44 ± 10.58	59.57 ± 12.88 ns	54.51 ± 8.23 ns	65.71 ± 5.18 **≠
(Tb.Th) (μm)	71.10 ± 18.66	51.98 ± 15.39 ***	61.73 ± 12.85 ns≠	40.93 ± 5.47 ***++
(Tb.N) (mm^{-1})	3.65 ± 0.56	5.95 ± 1.38 ***	5.3 ± 0.74 ***	5.6 ± 0.74 ***
(Tb.Sp) (μm)	84.21 ± 27.28	112.57 ± 24.59 *	117.41 ± 10.44 **	114.16 ± 20.50 **
(OS/BS) (%)	6.86 ± 1.88	3.95 ± 0.25 ***	3.05 ± 0.24 ***	3.19 ± 0.32 ***

BV/TV: Trabecular bone volume; Tb.Th: Trabecular thickness; Tb.N: Trabecular number; Tb.Sp: Intertrabecular distance; and OS/BS: Osteoid surface. Values were expressed as mean ± SD. The FW, PI, and FS groups differed significantly from the control group (* $p < 0.05$; ** $p < 0.01$; *** $p < 0.001$). The FW group differed significantly from the PI and FS groups (≠ $p < 0.05$). The PI group differed significantly from the FS group (++ $p < 0.01$) ns: not significant.

2.9. Multivariate Analysis Reveals Strong Associations Between Oxidative Stress and Bone Microarchitectural Alterations

To further explore the relationship between chronic stress-induced oxidative damage and bone microarchitectural alterations, a comprehensive multivariate approach combining Principal Component Analysis (PCA) and pairwise Spearman rank correlation analyses was performed.

With Principal Component 1 (PC1) accounting for 61.65% and PC2 for 12.50% of the total variance in the first two dimensions, the PCA effectively captured 74.14% of the overall variance (Table 3). Bone remodeling indicators and systemic oxidative stress were major drivers of PC1. MDA (+0.4138), ACP (+0.3714), H_2O_2 (+0.3702), and ROS (+0.3617) showed high positive loadings, whereas trabecular thickness Tb.Th (−0.2978) and the bone formation marker ALP (−0.3666) showed inverse loadings. On the other hand, PC2 was mostly determined by bone structural geometry, with notable positive loadings for Tb.Th (+0.5108) and BV/TV (+0.7594).

Table 3. Eigenvalues, variance proportions, and eigenvectors (loadings) for the first two principal components.

Metrics and Variables	PC1	PC2
Eigenvalue	5.5481	1.1248
Proportion of Variance	0.6165 (61.65%)	0.1250 (12.50%)
Cumulative Variance	0.6165 (61.65%)	0.7414 (74.14%)
Variable Loadings		
MDA	0.4138	0.0066
ROS	0.3617	−0.1337
H_2O_2	0.3702	0.1830
ALP	−0.3666	−0.1193
ACP	0.3714	0.0831
BV/TV	0.2056	0.7594
Tb.Th	−0.2978	0.5108
Tb.N	0.2439	−0.0300
Tb.Sp	0.3133	−0.2982

PC1: Principal Component 1; PC2: Principal Component 2.

The experimental groups were clearly separated based on their biological profiles when individual coordinates were projected onto the factor score plot (Figure S1, Supplementary Information; Table 3). Because of their well-preserved bone density and minimal systemic oxidation, the control group clearly grouped in the upper-left quadrant. The FW group, on the other hand, showed significant shifts along PC1 and was distinguished by increased oxidative stress indicators and bone resorption-related measures. While the FS group occupied an intermediate region and had a dual phenotypic impact, the PI group moved downward along PC2, segregated by a dominant structural deterioration pattern.

To complement the PCA and evaluate the overarching biological laws across all samples (n = 24), a pairwise Spearman rank correlation analysis was executed (Figure S2, Supplementary Information, Table 4).

Table 4. Spearman's rank correlation matrix (p) for the overall study population (n = 24).

Variables	MDA	ROS	H_2O_2	ALP	ACP	BV/TV	Tb.Th	Tb.N	Tb.Sp
MDA	1.000								
ROS	0.782 ***	1.000							
H_2O_2	0.915 ***	0.606 **	1.000						
ALP	−0.850 ***	−0.797 ***	−0.751 ***	1.000					
ACP	0.845 ***	0.755 ***	0.725 ***	−0.782 ***	1.000				
BV/TV	−0.510 *	0.248	−0.501 *	−0.442 *	0.510 *	1.000			
Tb.Th	−0.581 **	−0.480 *	−0.494 *	0.467 *	−0.581 **	−0.063	1.000		
Tb.N	−0.474 *	−0.412 *	−0.443 *	−0.327	0.385	0.150	−0.509 *	1.000	
Tb.Sp	0.592 **	0.447 *	0.543 **	−0.545 **	0.579 **	0.111	−0.666 ***	0.352	1.000

Values represent Spearman's rank correlation coefficients (ρ). Values indicate statistically significant correlations, with asterisks defining the exact level of significance: * $p < 0.05$, ** $p < 0.01$, *** $p < 0.001$.

Global Spearman correlation analysis showed that increased oxidative stress was structurally linked to the progressive degradation of bone microarchitecture. Systemic oxidative stress markers (MDA, ROS, and H_2O_2) were consistently and negatively associated with primary bone quality parameters, particularly BV/TV, Tb.Th, and Tb.N, while being positively associated with trabecular separation (Tb.Sp) (Table 4).

Remarkably, lipid peroxidation levels co-varied almost perfectly with H_2O_2 (p = 0.915, $p < 0.001$) and correlated negatively with Tb.Th (p = −0.581, p = 0.0029), whilst aligning positively with an increased Tb.Sp (p = 0.592, p = 0.0023).

Additionally, the hypothesis that increased oxidative stress is linked to an imbalance in bone remodeling, favoring resorptive activity, is supported by the strong inverse association between MDA and the bone-forming marker ALP (ρ = −0.850, $p < 0.001$) and the strong positive correlation between MDA and the bone-resorbing enzyme ACP (ρ = 0.845, $p < 0.001$).

To further dissect the specific impact of chronic stress exposure, a secondary stratified correlation analysis was restricted exclusively to the active stress cohorts (FW, PI, and FS; n = 18) to isolate the pathogenic trajectories from baseline control variations (Figure 7, Table 5). Within the stress-exposed groups, lipid peroxidation remained a powerful negative driver of functional bone volume, exhibiting a significant inverse correlation with BV/TV (p = −0.61, $p < 0.01$) and a strong negative coupling with H_2O_2 (p = −0.59, $p < 0.01$). This confirms that under active stress conditions, the intensity of the oxidative burst directly dictates the scale of trabecular bone loss. Concurrently, the tight synchronization between high MDA levels and the up-regulation of the bone-resorbing enzyme ACP was highly preserved (p = 0.87, $p < 0.001$), while remaining strongly antagonistic to the bone-forming marker ALP (p = −0.68, $p < 0.01$). Interestingly, when filtering out the controls, the independent variations in Tb.Th and Tb.N did not display direct linear associations with immediate oxidative indicators ($p > 0.05$). However, a localized positive correlation

was maintained between trabecular thickness and intertrabecular distance (Tb.Sp, $p = 0.51$, $p < 0.05$). Taken together, these intra-group observations support the hypothesis that oxidative imbalance contributes to stress-related bone deterioration, potentially through alterations in bone remodeling pathways characterized by enhanced resorptive activity and reduced bone formation.

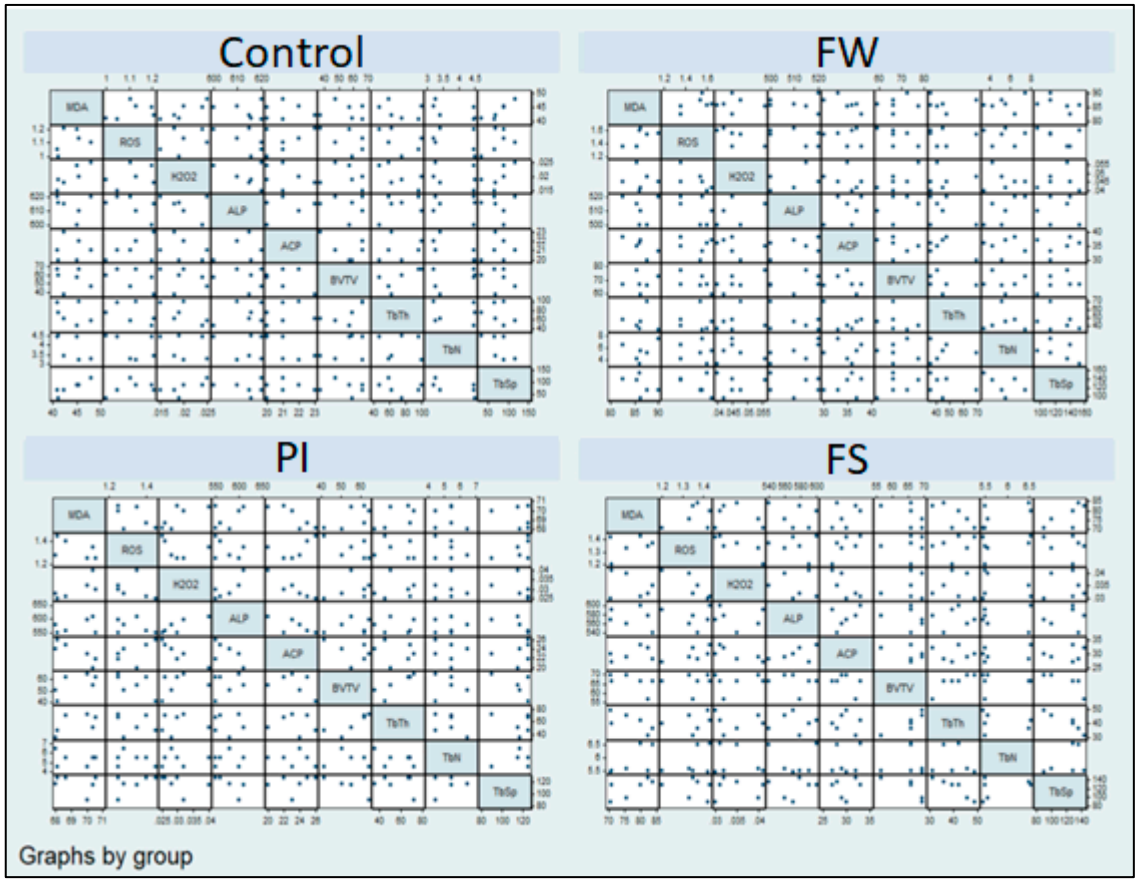


Figure 7. Stratified pairwise Spearman correlation matrix scatterplots across individual experimental groups. Multi-panel scatterplot matrix illustrating the bivariate relationships between oxidative biomarkers (MDA, ROS, and H_2O_2) and bone microarchitectural parameters (ALP, ACP, BV/TV, Tb.Th, Tb.N, and Tb.Sp) separated by experimental group: Control, food and water restriction (FW), permanent illumination (PI), and forced swimming (FS).

Table 5. Intra-group Spearman's rank correlation matrix (p) within the pooled stressed cohorts.

Variables	MDA	ROS	H_2O_2	ALP	ACP	BV/TV	Tb.Th	Tb.N	Tb.Sp
MDA	1.00								
ROS	0.54 *	1.00							
H_2O_2	0.81 ***	0.15	1.00						
ALP	−0.68 **	−0.58 *	−0.51 *	1.00					
ACP	0.87 ***	−0.56 *	−0.57 *	−0.61 **	1.00				
BV/TV	−0.61 **	−0.15	−0.59 **	0.43	−0.54 *	1.00			
Tb.Th	−0.32	−0.10	−0.12	−0.10	−0.37	0.05	1.00		
Tb.N	−0.06	−0.08	−0.03	0.24	−0.03	−0.01	0.35	1.00	
Tb.Sp	0.19	0.05	0.09	−0.18	−0.31	0.02	0.51	−0.01	1.00

Values represent Spearman's rank correlation coefficients (p) extracted from the combined stress treatment groups. Values indicate statistically significant associations: * $p < 0.05$, ** $p < 0.01$, *** $p < 0.001$.

3. Discussion

Bone remodeling is frequently maintained by osteoclast-mediated resorption and osteoblast-mediated refilling. ALP, a vital enzyme in bone remodeling, regulates calcium and phosphate deposition in the extracellular matrix [17]. Our results suggest increased bone resorption activity. In fact, compared with the controls, ACP activity was significantly higher, while ALP activity was lower. Reduced ALP activity may indicate poor bone formation, a feature commonly observed in metabolic bone disorders and osteoporosis [18]. Notably, this response was not uniform across models, as FW consistently showed the most marked alterations in bone resorption markers, whereas FS and PI induced progressively milder effects. Osteoclasts produce large levels of ROS during resorption, and when these ROS build up, they inhibit the production of new bone and promote more resorption [19,20].

In addition to changes in bone turnover markers, our three different stress conditions: food and water restriction, continuous exposure to light, and forced swimming, induced significant alterations in plasma and bone mineral composition.

Trace elements such as Cu, Zn, Fe, and Mn are essential for both antioxidant defense and bone metabolism. Their depletion may weaken antioxidant capacity and increase susceptibility to oxidative damage. Moreover, the decrease in circulating phosphorus levels, together with reduced bone tissue levels, suggests enhanced bone resorption and mobilization of skeletal mineral stores [19,21]. These alterations may result from stress-induced endocrine and metabolic disturbances and could contribute to the impaired bone remodeling observed in the present study. However, it is important to note that the observed mineral alterations may arise from different mechanisms under different stress conditions. Food withdrawal may directly decrease mineral intake, but forced swimming stress may affect mineral homeostasis through glucocorticoid production, oxidative stress, inflammatory processes, or altered renal mineral handling. The PI model is likely to induce neuroendocrine and metabolic alterations through hypothalamic–pituitary–adrenal axis activation, which is, in turn, driven by mineral redistribution, utilization, and excretion. Therefore, these stressor-specific pathways could contribute in different ways to mineral metabolism, especially phosphorus and calcium.

In the present study, plasma copper and zinc levels decreased, possibly due to their possible interaction with absorption [17]. As both elements are essential cofactors of Cu/Zn-SOD, their depletion may lead to decreased SOD activity, as observed in our study.

Catalase, a heme-containing antioxidant enzyme, acts sequentially with SOD in the conversion of hydrogen peroxide to water [22]. The active region of catalase has a ferric (Fe^{+3}) protoporphyrin group. However, as Cu is required for proper Fe utilization, Cu deficit can lower catalase activity. Therefore, the reduction in copper levels may be a potential factor contributing to the decrease in catalase activity observed in the treated groups [23]. O_2 production or a direct impact of labor stress exposure on enzyme synthesis could be the cause of GPx's decreased activity [24]. Similarly, essential components of the non-enzymatic antioxidant defense system, such as GSH, NPSH, and vitamin C, act as direct scavengers of ROS [25].

The reduction in these levels may reflect increased utilization of GSH and NPSH in response to oxidative challenge. Indeed, increased generation of free radicals, such as H_2O_2 and superoxide anions, by xanthine oxidase can deplete non-enzymatic antioxidants and interfere with osteoblast growth in mouse and rabbit marrow cells [26,27], while promoting osteoclast differentiation and bone resorption [28].

GSH helps recycle vitamin C by reducing dehydroascorbate; a lack of GSH may lead to lower vitamin C levels in the femurs of people under chronic stress. GSH and NPSH depletion indicate that excessive ROS production overwhelms antioxidant defenses, leading to oxidative stress and lipid peroxidation. Higher levels of MDA, H_2O_2, and LOOH in

groups linked to chronic stress supported these findings. Moreover, elevated AOPP and PCO levels in bone tissue indicate that increased ROS probably led to protein oxidation.

The skeletal alterations observed in the present study were associated with marked oxidative imbalance, as evidenced by increased oxidative damage markers and impaired antioxidant defenses. These findings are consistent with the recognized role of oxidative stress in bone remodeling, where excessive ROS promote osteoclast activity while impairing osteoblast function [29]. Multivariate studies were conducted to provide further evidence of the association between oxidative stress and bone degeneration. The FW group displayed the strongest correlation with oxidative stress indicators and abnormalities in bone remodeling. PCA effectively distinguished the experimental groups based on their skeletal and oxidative profiles. Elevated levels of MDA, ROS, H_2O_2, and ACP, along with ALP activity and trabecular thickness, were the primary factors driving the first principal component. This suggests a strong relationship between oxidative load and accelerated bone resorption.

Furthermore, substantial correlations were found between oxidative stress indicators and key microarchitectural characteristics of bone using Spearman's rank correlation analysis. Increased trabecular separation and decreased bone quality indices were often associated with elevated levels of MDA, ROS, and H_2O_2. The significant positive association between MDA and ACP, together with the negative association between MDA and ALP, further supports the hypothesis that oxidative damage induced by long-term stress shifts bone remodeling towards a resorptive phenotype. Overall, these results provide comprehensive statistical evidence that oxidative imbalance is a significant factor in stress-induced bone loss and microarchitectural degradation. However, the effects of chronic stress, especially under different stress conditions, on bone are likely multifactorial [30]. In addition to oxidative stress, activation of the hypothalamic–pituitary–adrenal axis and increased glucocorticoid secretion may contribute to reduced bone formation and enhanced resorption [31]. Furthermore, nutrient deprivation, circadian rhythm disruption induced by permanent illumination, and neuroendocrine responses associated with forced swimming may further influence bone metabolism. Taken together, these mechanisms support a possible contribution of chronic stress to bone alterations, which may result from interactions among oxidative, endocrine, and metabolic disturbances.

In the present study, food and water restriction, continuous light exposure, and the forced swimming stress paradigm induced an evident oxidative imbalance and alterations in bone tissue, but the stress mechanisms are not the same; they are specific to each stress model. Common findings across these three models included oxidative imbalance, ROS overproduction, and alterations in bone turnover and remodeling. These data and observations support the hypothesis that chronic stress, regardless of its origin or nature, may adversely affect bone homeostasis through oxidative stress and endocrine pathways. However, distinct features have been noted among the three paradigms models. The food and water restriction model induced the most pronounced decalcification and trabecular discontinuity. This observation reflects the combined effects of metabolic stress. Indeed, it is important to note that oxidative stress is likely not the only factor contributing to the increased severity observed in the FW group. Unlike other stress models, this one involves a direct reduction in the availability of essential nutrients and minerals, particularly calcium, phosphorus, and trace elements vital for bone metabolism. This caloric deficit can impair bone mineralization and remodeling on its own. Moreover, the FW group exhibited the highest oxidative stress and the most significant changes in antioxidant defenses, suggesting that oxidative damage may further exacerbate skeletal deterioration. Therefore, the substantial bone changes seen in FW animals are probably the result of a combination of factors, including oxidative stress, dietary deprivation, and stress-related hormonal

disorders, rather than a single underlying cause. In contrast, in the PI model, we showed alterations in mineralization patterns, probably due to circadian rhythm perturbation and its direct or indirect consequences on endocrine regulation. On the other hand, the FS model induced well-formed but basophilic trabeculae, suggesting impaired mineralization and probably sustained physical effects and ROS generation. These differences among the three models suggest that, while chronic stress may induce common detrimental effects on bone tissue, the underlying pathways, mechanisms, and resulting skeletal manifestations vary according to the type of stressor.

Histological investigations indicated abnormalities in bone production, as evidenced by changes in mineralization determined by the single-turnover rate. In the chronic-stress-exposed groups, the growth plate was highly disordered compared to the control group. The hypertrophic zone was significantly reduced and indistinct, and proliferating chondrocytes failed to form distinct columns. These changes may result from bone cytotoxicity caused by free-radical accumulation [28]. Our histological examination also revealed significant discontinuity of trabecular bone, decreased trabecular connectivity, and thinning, especially in the group denied food and drink. This discontinuity indicates significant decalcification. We observed well-developed trabeculae with black pigmentation in the stress lighting group, suggesting a mineralization issue. The swim stress group showed basophilic, well-formed trabeculae, suggesting a lack of mineralization.

Several factors influence the ratio of osteoblastic to osteoclastic activity. Stress, whether physical or psychological, can upset this equilibrium by causing hormonal and cellular alterations. Previous studies have suggested that prolonged stress may increase glucocorticoid secretion, which can negatively influence osteoblast function and favor bone resorption [32,33]. Consistent with this interpretation, in our previous studies using the same chronic-stress experimental model, we reported increased corticosterone levels and alterations in inflammatory markers [34,35]. These findings suggest that activation of stress-related endocrine responses and inflammatory pathways may contribute to the physiological and bone alterations observed under chronic stress conditions.

It is essential to emphasize that the stress paradigms utilized in this research highlight crucial biological aspects of chronic stress across various conditions, even though they are artificially intensified and do not directly replicate typical human experiences. For instance, continuous light exposure simulates ongoing circadian disruptions and sleep deprivation, which are common in shift workers, military personnel, and high-performance athletes. Similarly, the forced swimming model mimics long-term physical and mental strain, showing physiological similarities to chronic fatigue and overtraining syndrome. Moreover, food and water restriction represent a severe form of nutrient insufficiency and metabolic stress, reflecting poor nutritional intake, prolonged energy deficits, or adverse environmental conditions. Therefore, these models offer valuable mechanistic insights into how oxidative, endocrine, and metabolic abnormalities associated with chronic stress can adversely affect bone health. However, they should not be taken as direct representations of human stress exposure.

4. Materials and Methods

4.1. Reagents

All chemicals were of analytical grade and sourced from standard commercial suppliers. sodium ethylenediaminetetraacetate (Na_2EDTA), methionine, nitro blue tetrazolium (NBT), riboflavin, hydrogen peroxide (H_2O_2), potassium iodide (KI) solution, acetic acid, trichloroacetic acid (TCA), 2,4-dinitrophenylhydrazine (DNPH), copper sulfate ($CuSO_4$), sulfuric acid (H_2SO_4), and thiobarbituric acid (TBA) were purchased from Sigma-Aldrich (St. Louis, MO, USA).

4.2. Animals and the Development of Experimental Models of Stress

We used 24 healthy male Wistar rats (8–10 weeks old) weighing 150 ± 10 g. The animals were housed in pre-bedded polyethylene cages under standard laboratory conditions (25 ± 2 °C; 12 h light/dark cycle). Rats had ad libitum access to water and a standard pellet diet (SNA, Sfax, Tunisia).

All experimental procedures were conducted in compliance with European Union legislation on the protection of animals used for scientific purposes (Directive 2010/63/EU) and approved by the local ethics committee (Protocol No. 09.0010/22).

The rats were randomly allocated into four groups (n = 6 per group):

- Control group (Control): non-stressed animals maintained under standard laboratory conditions.
- FW group: exposed for to food and water restriction stress 21 days;
- PI group: subjected to permanent illumination stress for 21 days (24/7);
- FS group: exposed to forced swimming stress for 21 consecutive days.

4.2.1. Food and Water Deprivation Protocol

The experimental protocol was carried out in strict compliance with established guidelines for food and water restriction in rodent studies. During the 21-day experimental period, rats assigned to the food and water restriction group were subjected to a controlled restriction schedule. The amount of food and water provided was adjusted to approximately 70% of the average ad libitum consumption measured in control animals. Food and water were supplied at the same time each day, and intake was monitored throughout the experiment to ensure compliance with the protocol [36–40].

4.2.2. Permanent Illumination Protocol

Animals were exposed to continuous illumination (24 h/day) using a 100 W bulb placed 2.75 m above the center of the room, providing approximately 100 lx at floor level. Temperature was maintained between 24 and 27 °C. Food and water were provided ad libitum. Before the experiment, animals underwent a three-day acclimatization period to room conditions and the light cycle without handling [41].

4.2.3. Forced Swim Protocol

Rats underwent 20 days of forced swim stress sessions (4 days/5) as part of the forced swim regimen [13]. Rats were individually placed in the water-filled forced swim tank for 15 min every day throughout this time. Each rat was made to swim in a vertical borosilicate glass jar (25 cm × 12 cm × 25 cm) filled with water at 23 ± 1 °C. The rat's size was taken into consideration while adjusting the water depth to prevent its hind legs from touching the bottom of the container. The rats were quite busy when they were originally put in the jar, swimming in circles and attempting to climb the walls or dive to the bottom. The rats were removed from the water after 15 min, dried with a dry cloth, and returned to their cages. After testing for every rat, the jar was emptied and carefully cleaned.

Animal health and welfare were monitored daily throughout the experimental period. Body weight, food intake, water consumption, general appearance, locomotor activity, and signs of distress were recorded regularly. Humane endpoints were predefined according to institutional ethical guidelines and included severe weight loss, persistent inactivity, inability to access food or water, or signs of severe suffering. No animals reached the predefined humane endpoints during the study period.

4.3. Anesthesia

After 21 days, animals from each group were anesthetized intramuscularly with ketamine 50 mg/mL (200 µL) and midazolam 5 mg/mL (20 µL), then euthanized, as described by Hamdaoui et al. [42].

4.4. Plasma Preparation

Blood samples were collected in heparin tubes, centrifuged at 2500× *g* for 15 min, and the plasma was aliquoted immediately after centrifugation and stored at −80 °C until analysis. Repeated freeze–thaw cycles were avoided.

4.5. Mineral Content in Plasma and Femurs

Iron (Fe), magnesium (Mg), zinc (Zn), copper (Cu), calcium (Ca), and phosphorus (P) were measured following nitroperchloric mineralization using atomic absorption spectroscopy (Thermo-Scientific ICE 3000, Sherwood Scientific Ltd., Cambridge, UK). The wavelengths used for analysis were as follows: Fe (248.3 nm), Zn (213.9 nm), Cu (324.8 nm), Mg (285.2 nm), and Ca (422.7 nm). The detection limits of the atomic absorption spectrometer were within the manufacturer's recommended specifications for Fe, Zn, Cu, Mg, and Ca analyses.

4.6. Plasma Total Alkaline Phosphatase (ALP) and Acid Phosphatase (ACP) Levels

The ALP and ACP plasma levels were determined by colorimetric methods from Elitech Diagnostics (Sees, France; Ref. PASL-0500) and bioMérieux (Marcy-l'Étoile, France; Ref. 746419901).

4.7. Bone Sample Preparation

Following sacrifice, the femurs were dissected, and the surrounding muscles were promptly removed. The femurs were weighed, with some used for histological examination and others stored at −80 °C for biochemical assays.

4.8. Bone Sample Preparation for Biochemical Assays

A total of 100 mg of bone samples was homogenized with 2 mL of 0.1 M Tris–HCl buffer (pH 7.2) using a mortar and pestle [43]. The homogenates were centrifuged at 10,000× *g* for 30 min at 4 °C. The supernatants were aliquoted and stored at −80 °C until biochemical analyses. All assays were performed within one week of sample collection to minimize analyte degradation.

4.9. Protein Quantification

Bone protein levels were quantified using bovine serum albumin, as previously described by Lowry et al. [44]. Protein concentrations were used to normalize all oxidative stress and antioxidant biomarkers measured in bone homogenates. Results were therefore expressed relative to total protein content to minimize variations related to tissue processing and extraction efficiency.

4.10. Measurement of Lipid Peroxidation and Lipid Hydroperoxides (LOOHs)

The bone malondialdehyde (MDA) levels were assayed spectrophotometrically using the Draper and Hadley method [45]. The MDA values were calculated using 1,1,3,3-tetraethoxypropane as a standard and expressed as nanomoles of MDA/mg protein. Standard curves were prepared using 1,1,3,3-tetraethoxypropane, and sample concentrations were calculated from the corresponding calibration curve.

LOOHs were measured using the ferrous oxidation in xylenol orange (FOX) assay, as described by Jiang et al. [46]. Results were expressed as nanomoles per milligram of protein.

4.11. Determination of Bone Advanced Oxidation Protein Products (AOPP) Levels

AOPP levels were measured in reference to the method of Kayali et al. [47]. The levels of AOPP were calculated using the extinction coefficient of 261 cm^{-1} mM^{-1} and expressed as nanomoles/mg protein.

4.12. Determination of Protein Carbonyl (PCO) Levels in Bone

PCO contents were determined using the Reznick and Packer's method [48]. The carbonyl levels were calculated based on the molar extinction coefficient of DNPH ($e = 2.2 \times 10^4$ cm^{-1} M^{-1}) and expressed as μmoles/mg of protein.

4.13. Measurement of Reactive Oxygen Species (ROS) Generation

ROS levels were measured using 2′,7′-dichlorofluorescein diacetate (DCFH-DA) according to a previously described protocol [49,50]. Arbitrary units, expressed as relative fluorescence units (FU), were based directly on fluorescence intensity. The data were expressed as FU per minute per mg protein.

4.14. Measurement of Hydrogen Peroxide (H_2O_2) in Bone Tissue

H_2O_2 was determined, following the method described by Ou et al. [51]. H_2O_2 levels were expressed as μmoles/mg protein.

4.15. Determination of Antioxidant Defense in Bone Tissue

Bone superoxide dismutase (SOD) activity was assayed according to the method of Beauchamp et al. [52]. SOD activity was expressed as the amount of enzyme required to inhibit the reduction in NBT by 50%, and the activity was reported as units/mg of protein.

Bone glutathione peroxidase (GPx) activity was measured as described by Flohé and Günzler [53]. GPx activity was expressed as nanomoles of GSH oxidized/min/mg of protein.

Bone catalase (CAT) activity was assayed by Aebi's method [54]. CAT activity was calculated as μmoles of H_2O_2 consumed/min/mg of protein.

Bone glutathione (GSH) level was determined by the method of Jollow et al. [18]. Total GSH content was expressed as μg/mg of protein.

Bone non-protein sulfhydryl (NPSH) levels were determined using Ellman's method [19]. NPSH content was expressed as μmoles/mg of protein.

Bone vitamin C was determined as described by Jacques-Silva et al. [21]. The data were expressed as μmoles of ascorbic acid/mg of protein.

4.16. Histological Studies

Femurs intended for histological examination were collected and immediately demineralized for 72 h in acetic acid (1.7 mol/L) at room temperature as described by Talbott et al. [20]. They were then fixed for 48 h in 10% formalin, embedded in paraffin, serially sectioned at 5 μm, and stained with hematoxylin–eosin (H-E) for light microscopy.

4.17. Scanning Electron Microscopy (SEM)

SEM was performed on the femurs of treated rats. Briefly, the femurs were longitudinally sectioned and immersed in 50% sodium hypochlorite to remove organic material. After 3 h, bone samples were rinsed three times with distilled water and then fixed overnight in 1% osmium tetroxide. Subsequently, the samples were rinsed for 30 min with distilled

water and then dehydrated in an ascending ethanol series (70, 95, and 100%). Finally, the samples were heated for 1 h in hexamethyl disilazane and then air-dried on filter paper. SEM was performed at 20 kV using a scanning electron microscope (JEOL JSM-5100, JEOL Ltd., Tokyo, Japan).

4.18. Histomorphometric Analysis of Bone Samples

Trabecular bone volume (BV/TV, expressed in %), Trabecular thickness (Tb.Th, expressed in μm), Trabecular number (Tb.N, expressed in mm^{-1}), Intertrabecular distance (Tb.Sp, expressed in μm), Osteoid surface (OS/BS, expressed in %) were measured. The osteoid surface was primarily based on the percentage of the endosteal bone surface and showed features of bone resorption with osteoclasts (OCs). Histomorphometric analysis of rat femurs was performed using ImageJ 1.48v software. The same investigator performed histomorphometric measurements under blinded conditions. For each animal, measurements were obtained from at least three non-overlapping microscopic fields and averaged to obtain a representative value [21].

4.19. Quality Control and Assay Validation

All biochemical analyses were performed using freshly prepared reagents according to validated published protocols. Measurements were conducted in duplicate, and calibration standards and blank controls were included in each assay. Plasma and bone homogenate samples were stored at −80 °C until analysis, and repeated freeze–thaw cycles were avoided. Instrument calibration for mineral determination was performed according to the manufacturer's recommendations, and all measurements were conducted within the linear detection range of the respective assays. For biochemical measurements, quality control samples were analyzed in parallel with experimental samples. The intra-assay and inter-assay coefficients of variation were maintained below 10 and 15%, respectively.

4.20. Statistical Analysis

Statistical analysis was performed using SPSS software (version 26; SPSS Inc., Chicago, IL, USA). Parametric quantitative data were presented as mean ± standard deviation (SD) and analyzed using one-way ANOVA followed by Tukey's post hoc test. A p-value of less than 0.05 was considered statistically significant.

To explore global phenotypic patterns and find dependencies across multiple variables, a multivariate Principal Component Analysis (PCA) based on the correlation matrix was executed. Bivariate relationships between systemic oxidative stress biomarkers, and bone histomorphometric parameters were evaluated using non-parametric Spearman's rank correlation analysis (p) to successfully capture both overall population (n = 24) and intra-group (n = 18, stratified by stress conditions) monotonic trends. The PCA and Spearman correlation analyses, including the generation of scatterplot matrices, were performed using Stata software (version 12.0; StataCorp, College Station, TX, USA). For all statistical tests, a p-value of less than 0.05 was considered statistically significant (* $p < 0.05$, ** $p < 0.01$, *** $p < 0.001$).

5. Conclusions

In summary, chronic stress poses a significant risk to bone health. It causes oxidative damage, as evidenced by elevated lipid peroxidation and reduced antioxidant capacity. It was associated with alterations in bone mineral composition and bone microarchitecture. These findings show how chronic stress affects bone health. This study has several limitations, including the use of an animal model that may not fully replicate human chronic stress, the relatively short duration of stress exposure, and the lack of molecular pathway analyses to elucidate further the mechanisms underlying the observed effects.

Therefore, larger-scale studies are needed to confirm the mechanisms underlying chronic stress exposure.

Supplementary Materials: The following supporting information can be downloaded at https://www.mdpi.com/article/10.3390/physiologia6030046/s1, Figure S1: Principal Component Analysis (PCA) with the distinct biological profiles of Control, FW, PI, and FS groups. Figure S2: Pairwise Spearman correlation analysis between oxidative stress and bone structural parameters.

Author Contributions: Conceptualization, J.M.P., L.H. and I.B.A.; methodology, J.M.P., M.L. and I.B.A.; software, M.L. and D.Y.F.; validation, J.M.P., H.B.S., H.K. and I.B.A.; formal analysis, J.M.P. and M.L.; investigation, J.M.P., L.H., M.L., O.B., T.B. and M.K.; resources, H.B.S., H.K. and I.B.A.; data curation, M.L., D.Y.F. and I.B.A.; writing—original draft preparation, J.M.P., L.H. and M.L.; writing—review and editing, H.B.S., H.K. and I.B.A.; visualization, M.L. and D.Y.F.; supervision, H.K. and I.B.A.; project administration, I.B.A.; funding acquisition, H.K. and I.B.A. All authors have read and agreed to the published version of the manuscript.

Funding: This work was supported by the French Guiana University Hospital—Cayenne Site.

Institutional Review Board Statement: The animal study protocol was approved by the local ethics committee (Protocol No. 09.0010/22; 9 October 2022).

Informed Consent Statement: Not applicable for this study.

Data Availability Statement: The raw data supporting the conclusions of this article will be made available by the authors on request.

Acknowledgments: The authors would like to express their gratitude to Thomas Rugi and Amandine Papin for their logistical support in carrying out this study. We highly appreciate Mathieu Nacher for his thorough review and validation of the multivariate and correlation analyses carried out with Stata 12.

Conflicts of Interest: The authors declare no conflicts of interest.

References

1. Baron, R.; Hesse, E. Update on Bone Anabolics in Osteoporosis Treatment: Rationale, Current Status, and Perspectives. *J. Clin. Endocrinol. Metab.* **2012**, *97*, 311–325. [CrossRef] [PubMed]
2. Feng, X.; McDonald, J.M. Disorders of Bone Remodeling. *Annu. Rev. Pathol.* **2011**, *6*, 121–145. [CrossRef] [PubMed]
3. Dirckx, N.; Moorer, M.C.; Clemens, T.L.; Riddle, R.C. The Role of Osteoblasts in Energy Homeostasis. *Nat. Rev. Endocrinol.* **2019**, *15*, 651–665. [CrossRef] [PubMed]
4. Robling, A.G.; Bonewald, L.F. The Osteocyte: New Insights. *Annu. Rev. Physiol.* **2020**, *82*, 485–506. [CrossRef] [PubMed]
5. Nekrasova, M.R.; Suplotova, L.A.; Davydova, L.I. The problem of osteopenia in a iodine-deficit area. *Klin. Med.* **2006**, *84*, 62–65.
6. Moreno-Reyes, R.; Egrise, D.; Boelaert, M.; Goldman, S.; Meuris, S. Iodine Deficiency Mitigates Growth Retardation and Osteopenia in Selenium-Deficient Rats. *J. Nutr.* **2006**, *136*, 595–600. [CrossRef] [PubMed]
7. Ren, F.L.; Guo, X.; Zhang, R.J.; Wang, S.J.; Zuo, H.; Zhang, Z.T.; Geng, D.; Yu, Y.; Su, M. Effects of Selenium and Iodine Deficiency on Bone, Cartilage Growth Plate and Chondrocyte Differentiation in Two Generations of Rats. *Osteoarthr. Cartil.* **2007**, *15*, 1171–1177. [CrossRef] [PubMed]
8. Das, K.; Chainy, G.B.N. Thyroid Hormone Influences Antioxidant Defense System in Adult Rat Brain. *Neurochem. Res.* **2004**, *29*, 1755–1766. [CrossRef] [PubMed]
9. Ben Amara, I.; Troudi, A.; Soudani, N.; Guermazi, F.; Zeghal, N. Toxicity of Methimazole on Femoral Bone in Suckling Rats: Alleviation by Selenium. *Exp. Toxicol. Pathol.* **2012**, *64*, 187–195. [CrossRef] [PubMed]
10. Akman, C.; Zhao, Q.; Liu, X.; Holmes, G.L. Effect of Food Deprivation during Early Development on Cognition and Neurogenesis in the Rat. *Epilepsy Behav.* **2004**, *5*, 446–454. [CrossRef] [PubMed]
11. Escribano, B.M.; Díaz-Moreno, A.; Tasset, I.; Túnez, I. Impact of Light/Dark Cycle Patterns on Oxidative Stress in an Adriamycin-Induced Nephropathy Model in Rats. *PLoS ONE* **2014**, *9*, e97713. [CrossRef] [PubMed]
12. de Kloet, E.R.; Molendijk, M.L. Coping with the Forced Swim Stressor: Towards Understanding an Adaptive Mechanism. *Neural Plast.* **2016**, *2016*, 6503162. [CrossRef] [PubMed]
13. Kawabe, K. Effects of Chronic Forced-Swim Stress on Behavioral Properties in Rats with Neonatal Repeated MK-801 Treatment. *Pharmacol. Biochem. Behav.* **2017**, *159*, 48–54. [CrossRef] [PubMed]

14. Mungenast, H.K.; Fox, A.E. Impact of Light–Dark Phase on Delay Discounting Behavior in Rats. *Psychol. Rec.* **2022**, *72*, 159–166. [CrossRef]
15. Dietze, S.; Lees, K.R.; Fink, H.; Brosda, J.; Voigt, J.-P. Food Deprivation, Body Weight Loss and Anxiety-Related Behavior in Rats. *Animals* **2016**, *6*, 4. [CrossRef] [PubMed]
16. Delorme, T.C.; Srikanta, S.B.; Fisk, A.S.; Cloutier, M.-È.; Sato, M.; Pothecary, C.A.; Merz, C.; Foster, R.G.; Brown, S.A.; Peirson, S.N.; et al. Chronic Exposure to Dim Light at Night or Irregular Lighting Conditions Impact Circadian Behavior, Motor Coordination, and Neuronal Morphology. *Front. Neurosci.* **2022**, *16*, 855154. [CrossRef] [PubMed]
17. Strissel, K.J.; Stancheva, Z.; Miyoshi, H.; Perfield, J.W.; DeFuria, J.; Jick, Z.; Greenberg, A.S.; Obin, M.S. Adipocyte Death, Adipose Tissue Remodeling, and Obesity Complications. *Diabetes* **2007**, *56*, 2910–2918. [CrossRef] [PubMed]
18. Jollow, D.J.; Mitchell, J.R.; Zampaglione, N.; Gillette, J.R. Bromobenzene-Induced Liver Necrosis. Protective Role of Glutathione and Evidence for 3,4-Bromobenzene Oxide as the Hepatotoxic Metabolite. *Pharmacology* **1974**, *11*, 151–169. [CrossRef] [PubMed]
19. Ellman, G.L. Tissue Sulfhydryl Groups. *Arch. Biochem. Biophys.* **1959**, *82*, 70–77. [CrossRef] [PubMed]
20. Talbott, S.M.; Cifuentes, M.; Dunn, M.G.; Shapses, S.A. Energy Restriction Reduces Bone Density and Biomechanical Properties in Aged Female Rats. *J. Nutr.* **2001**, *131*, 2382–2387. [CrossRef] [PubMed]
21. Jacques-Silva, M.C.; Nogueira, C.W.; Broch, L.C.; Flores, E.M.; Rocha, J.B. Diphenyl Diselenide and Ascorbic Acid Changes Deposition of Selenium and Ascorbic Acid in Liver and Brain of Mice. *Pharmacol. Toxicol.* **2001**, *88*, 119–125. [CrossRef] [PubMed]
22. Vimalraj, S. Alkaline Phosphatase: Structure, Expression and Its Function in Bone Mineralization. *Gene* **2020**, *754*, 144855. [CrossRef] [PubMed]
23. Lim, Z.W.; Chen, W.-L. Exploring the Association of Bone Alkaline Phosphatases and Hearing Loss. *Sci. Rep.* **2020**, *10*, 4006. [CrossRef] [PubMed]
24. Arai, M.; Shibata, Y.; Pugdee, K.; Abiko, Y.; Ogata, Y. Effects of Reactive Oxygen Species (ROS) on Antioxidant System and Osteoblastic Differentiation in MC3T3-E1 Cells. *IUBMB Life* **2007**, *59*, 27–33. [CrossRef] [PubMed]
25. Tolba, M.F.; El-Serafi, A.T.; Omar, H.A. Caffeic Acid Phenethyl Ester Protects against Glucocorticoid-Induced Osteoporosis in Vivo: Impact on Oxidative Stress and RANKL/OPG Signals. *Toxicol. Appl. Pharmacol.* **2017**, *324*, 26–35. [CrossRef] [PubMed]
26. Baek, K.H.; Oh, K.W.; Lee, W.Y.; Lee, S.S.; Kim, M.K.; Kwon, H.S.; Rhee, E.J.; Han, J.H.; Song, K.H.; Cha, B.Y.; et al. Association of Oxidative Stress with Postmenopausal Osteoporosis and the Effects of Hydrogen Peroxide on Osteoclast Formation in Human Bone Marrow Cell Cultures. *Calcif. Tissue Int.* **2010**, *87*, 226–235. [CrossRef] [PubMed]
27. Rowin, J. Copper Deficiency Myeloneuropathy and Pancytopenia Secondary to Overuse of Zinc Supplementation. *J. Neurol. Neurosurg. Psychiatry* **2005**, *76*, 750–751. [CrossRef] [PubMed]
28. Garrett, I.R.; Boyce, B.F.; Oreffo, R.O.; Bonewald, L.; Poser, J.; Mundy, G.R. Oxygen-Derived Free Radicals Stimulate Osteoclastic Bone Resorption in Rodent Bone in Vitro and in Vivo. *J. Clin. Investig.* **1990**, *85*, 632–639. [CrossRef] [PubMed]
29. Almeida, M.; Han, L.; Ambrogini, E.; Bartell, S.M.; Manolagas, S.C. Oxidative Stress Stimulates Apoptosis and Activates NF-kappaB in Osteoblastic Cells via a PKCbeta/P66shc Signaling Cascade: Counter Regulation by Estrogens or Androgens. *Mol. Endocrinol.* **2010**, *24*, 2030–2037. [CrossRef] [PubMed]
30. Manolagas, S.C. From Estrogen-Centric to Aging and Oxidative Stress: A Revised Perspective of the Pathogenesis of Osteoporosis. *Endocr. Rev.* **2010**, *31*, 266–300. [CrossRef] [PubMed]
31. Domazetovic, V.; Marcucci, G.; Iantomasi, T.; Brandi, M.L.; Vincenzini, M.T. Oxidative Stress in Bone Remodeling: Role of Antioxidants. *Clin. Cases Miner. Bone Metab.* **2017**, *14*, 209–216. [CrossRef] [PubMed]
32. Bădilă, A.E.; Rădulescu, D.M.; Ilie, A.; Niculescu, A.-G.; Grumezescu, A.M.; Rădulescu, A.R. Bone Regeneration and Oxidative Stress: An Updated Overview. *Antioxidants* **2022**, *11*, 318. [CrossRef] [PubMed]
33. Zhu, C.; Shen, S.; Zhang, S.; Huang, M.; Zhang, L.; Chen, X. Autophagy in Bone Remodeling: A Regulator of Oxidative Stress. *Front. Endocrinol.* **2022**, *13*, 898634. [CrossRef] [PubMed]
34. Pujo, J.M.; Fitriani, D.Y.; Ben Saad, H.; Ghariani, M.; Dghim, A.; Mellouli, M.; Burin, A.; Mutricy, R.; Houcke, S.; Roujansky, A.; et al. The Effects of Prolonged Stress Exposure on the Brain of Rats and Insights to Understand the Impact of Work-Related Stress on Caregivers. *Front. Behav. Neurosci.* **2023**, *17*, 1288814. [CrossRef] [PubMed]
35. Pujo, J.M.; Fitriani, D.Y.; Feki, A.; Kallabi, F.; Lakhrem, M.; Elleuch, A.; Kallel, C.; Roujansky, A.; Lontsi, G.R.; Houcke, S.; et al. Early Biomarkers of Occupational Strain in Caregivers: The Role of Inflammatory, Hematological, and Oxidative Stress Markers in Diagnosis. *Sci. Afr.* **2025**, *29*, e02861. [CrossRef]
36. Kant, G.J.; Yen, M.H.; D'Angelo, P.C.; Brown, A.J.; Eggleston, T. Maze Performance: A Direct Comparison of Food vs. Water Mazes. *Pharmacol. Biochem. Behav.* **1988**, *31*, 487–491. [CrossRef] [PubMed]
37. Voigt, J.-P.; Huston, J.P.; Voits, M.; Fink, H. Effects of Cholecystokinin Octapeptide (CCK-8) on Food Intake in Adult and Aged Rats under Different Feeding Conditions. *Peptides* **1996**, *17*, 1313–1315. [CrossRef] [PubMed]
38. Bert, B.; Harms, S.; Langen, B.; Fink, H. Clomipramine and Selegiline: Do They Influence Impulse Control? *J. Vet. Pharmacol. Ther.* **2006**, *29*, 41–47. [CrossRef] [PubMed]

39. Carlini, V.P.; Martini, A.C.; Schiöth, H.B.; Ruiz, R.D.; Fiol de Cuneo, M.; de Barioglio, S.R. Decreased Memory for Novel Object Recognition in Chronically Food-Restricted Mice Is Reversed by Acute Ghrelin Administration. *Neuroscience* **2008**, *153*, 929–934. [CrossRef] [PubMed]
40. Conrad, C.D. A Critical Review of Chronic Stress Effects on Spatial Learning and Memory. *Prog. Neuropsychopharmacol. Biol. Psychiatry* **2010**, *34*, 742–755. [CrossRef] [PubMed]
41. Dauchy, R.T.; Dauchy, E.M.; Hanifin, J.P.; Gauthreaux, S.L.; Mao, L.; Belancio, V.P.; Ooms, T.G.; Dupepe, L.M.; Jablonski, M.R.; Warfield, B.; et al. Effects of Spectral Transmittance through Standard Laboratory Cages on Circadian Metabolism and Physiology in Nude Rats. *J. Am. Assoc. Lab. Anim. Sci.* **2013**, *52*, 146–156. [PubMed]
42. Hamdaoui, L.; Oudadesse, H.; Lefeuvre, B.; Mahmoud, A.; Naifer, M.; Badraoui, R.; Ayadi, F.; Rebai, T. Sub-Chronic Exposure to Kalach 360 SL, Glyphosate-Based Herbicide, Induced Bone Rarefaction in Female Wistar Rats. *Toxicology* **2020**, *436*, 152412. [CrossRef] [PubMed]
43. Ramajayam, G.; Sridhar, M.; Karthikeyan, S.; Lavanya, R.; Veni, S.; Vignesh, R.C.; Ilangovan, R.; Djody, S.S.; Gopalakrishnan, V.; Arunakaran, J.; et al. Effects of Aroclor 1254 on Femoral Bone Metabolism in Adult Male Wistar Rats. *Toxicology* **2007**, *241*, 99–105. [CrossRef] [PubMed]
44. Lowry, O.H.; Rosebrough, N.J.; Farr, A.L.; Randall, R.J. Protein Measurement with the Folin Phenol Reagent. *J. Biol. Chem.* **1951**, *193*, 265–275. [CrossRef] [PubMed]
45. Draper, H.H.; Hadley, M. [43] Malondialdehyde Determination as Index of Lipid Peroxidation. In *Methods in Enzymology*; Elsevier: Amsterdam, The Netherlands, 1990; Volume 186, pp. 421–431, ISBN 978-0-12-182087-9.
46. Jiang, Z.Y.; Hunt, J.V.; Wolff, S.P. Ferrous Ion Oxidation in the Presence of Xylenol Orange for Detection of Lipid Hydroperoxide in Low Density Lipoprotein. *Anal. Biochem.* **1992**, *202*, 384–389. [CrossRef] [PubMed]
47. Kayali, R.; Çakatay, U.; Akçay, T.; Altuğ, T. Effect of Alpha-Lipoic Acid Supplementation on Markers of Protein Oxidation in Post-Mitotic Tissues of Ageing Rat. *Cell Biochem. Funct.* **2006**, *24*, 79–85. [CrossRef] [PubMed]
48. Reznick, A.Z.; Packer, L. [38] Oxidative Damage to Proteins: Spectrophotometric Method for Carbonyl Assay. In *Methods in Enzymology*; Elsevier: Amsterdam, The Netherlands, 1994; Volume 233, pp. 357–363, ISBN 978-0-12-182134-0.
49. Gerhardt, P. (Ed.) *Methods for General and Molecular Bacteriology*; American Society for Microbiology: Washington, DC, USA, 1994; ISBN 978-1-55581-048-1.
50. Shinomol, G.K. Muralidhara Differential Induction of Oxidative Impairments in Brain Regions of Male Mice Following Subchronic Consumption of Khesari Dhal (*Lathyrus sativus*) and Detoxified Khesari Dhal. *NeuroToxicology* **2007**, *28*, 798–806. [CrossRef] [PubMed]
51. Ou, P.; Wolff, S.P. A Discontinuous Method for Catalase Determination at "near Physiological" Concentrations of H2O2 and Its Application to the Study of H2O2 Fluxes within Cells. *J. Biochem. Biophys. Methods* **1996**, *31*, 59–67. [CrossRef] [PubMed]
52. Beauchamp, C.; Fridovich, I. Superoxide Dismutase: Improved Assays and an Assay Applicable to Acrylamide Gels. *Anal. Biochem.* **1971**, *44*, 276–287. [CrossRef] [PubMed]
53. Flohé, L.; Günzler, W.A. Assays of Glutathione Peroxidase. *Methods Enzymol.* **1984**, *105*, 114–121. [CrossRef] [PubMed]
54. Aebi, H. Catalase in Vitro. *Methods Enzymol.* **1984**, *105*, 121–126. [CrossRef] [PubMed]

Disclaimer/Publisher's Note: The statements, opinions and data contained in all publications are solely those of the individual author(s) and contributor(s) and not of MDPI and/or the editor(s). MDPI and/or the editor(s) disclaim responsibility for any injury to people or property resulting from any ideas, methods, instructions or products referred to in the content.